



Effect of Fin Parameters in Cylindrical and Divergent Duct under Natural Convection

S. Benkherbache^{1†} and M. Si-Ameur²

¹*Mechanical Engineering Department, University of M'sila, Algeria*

²*Laboratory of the Industrials Energy Systems studies, University of Batna, Algeria*

†*Corresponding Author Email: Souad.benkherbache@univ-msila.dz*

(Received March 26, 2018; accepted December 2, 2018)

ABSTRACT

In this paper we propose a numerical study of the natural convective heat transfer flow in a three dimensional cylindrical and divergent annular duct. The inner cylinder subjected to a volumetric heat generation is fitted with longitudinal fins. The governing equations of mass, momentum and energy equation for both the fluid and the solid are solved by the finite volume method, using the commercially available CFD software Fluent. The effect of the inclination angle ϕ of the divergent and the fin parameters on the profiles and the contour fields of temperature and velocity as well as the average Nusselt number ratio were investigated for $\phi=0^\circ, 15^\circ, 23^\circ$ and 45° and a number of fins, $N=1, 2, 3$ and 4 . The Simulations were carried out in the range of Rayleigh numbers ($Ra = 100$ to $Ra=6.3 \times 10^4$). The results reveal that the increasing of the inclination angle of the divergent and the number of fins enhances the heat transfer.

Keywords: Fin; Annular space; Divergent duct; Heat sink.

NOMENCLATURE

A_b	finned surface area	Q_{tot}	total heat transfer rate
A_c	cross sectional area of the fin	Ra	rayleigh Number
A_f	fin area	R_f	radius of the fin
C_p	specific heat	R_{ii}	radius of inner cylinder
D	characteristic length	R_{oi}, R_{oo}	radius of the inlet outer, outlet outer cylinder
D_h	hydraulic diameter	R_{th}	thermal resistance
g	gravitational acceleration	T_b	bulk temperature
H	height of the fin	u, v, w	components of velocity
h_{avg}	convective heat transfer coefficient	α	thermal diffusivity
$k_{f,s}$	thermal conductivity of fluid, solid	β	coefficient of thermal expansion
L	length of the duct	γ	angle between the fins
N	Fin number	δ	gap of annulus at inlet
NNR	average Nusselt number ratio	η	fin efficiency
Nu	Nusselt number	θ	angular coordinate
\overline{Nu}	average Nusselt number	μ	dynamic viscosity
P	pressure	ν	kinematic viscosity
Pr	prandtl number	ρ	fluid density
Q_b	Convective heat transfer rate	ϕ	inclination angle of the divergent
Q_f	fin heat transfer rate		

1. INTRODUCTION

Natural convection cooling with the help of the finned surfaces often offers an economical and free solution in many situations. Fines are used in a variety of engineering applications to dissipate heat to the surroundings. They also find applications in

electronics equipment like a heat sink. A heat sink is a passive heat exchanger that transfers thermal energy from a higher temperature device to a lower temperature fluid medium. The common configurations of naturally cooled heat sink are vertical and horizontal plates according to their geometry and applications such as plate heat sinks or

radial heat sinks. Radial heat sinks are used with high-power semiconductor devices such as power transistors and optoelectronics such as lasers and light emitting diodes (LED).

In a great number of relating studies, circular or rectangular base with various fin configurations have been extensively considered by researchers. In an experimental investigation, (Starner & McManus, 1963) measured the average heat transfer coefficient of four heat sinks of differing vertically, at 45° and horizontally. (Toshio, 1970). presented a study to obtain a reasonable method for predicting the characteristics of non-isothermal fin arrays with isothermal base-plates and good agreements between theoretical predictions and experiment were obtained. (Kumar, 1997) studied numerically the natural convection of stationary and laminar flow between two vertical cylinders fitted with longitudinal fins, he established two correlations of the Nusselt number and the angle between the fins as function of the Reynolds number and the thermal conductivities ratio. (An, Kim, & Kim, 2012) proposed a correlation to estimate the Nusselt number for natural convection from cylinders with vertically oriented plate fins. Experimental investigations for a radial heat sink also have been made by (Yu, Jang, & Lee, 2012; Yu, Lee, & Yook, 2010, 2011)) to propose a correlation for predicting the average Nusselt number and to examine the effect of radiation in the total heat transfer. (Li & Byon, 2015) investigated experimentally and numerically, the orientation effect on the thermal performance of radial heat sinks with a circular base. They proposed a closed-form correlation with associated orientation effect factor for predicting Nusselt number. Although, the divergent annular configuration is proposed for enhancing thermal performances of devices heat transfer, it has not been well investigated as compared to annular cylinder. To our knowledge, no studies have been found in the literature on natural convection in finned divergent annular duct. The present study considers, annular cylindrical and divergent duct fitted with fins. The present research was undertaken to continue the work reported in reference (Benkherbache & Si-Ameur, 2016) by studying the effects of various parameters such as inclination angle (ϕ) of the divergent, number of fins (N), inclination angle between fins (γ) and the height of the fins (H) on the flow pattern and heat transfer in the annular space.

2. FORMULATION OF THE PROBLEM

Figure 1 depicts the geometry of a three-dimensional (3D) steady laminar flow in vertical divergent annular duct, which inner cylinder is fitted with fins and subjected to uniform volumetric heat generation. The outer cylinder is inclined to form the divergent configuration and is supposed adiabatic. The duct is fully divided into equal sections to reduce the computational domain to the half volume. The fluid enters from the bottom of the duct with initial velocity w_0 and at ambient temperature T_0 . The top of the annular space is open to the atmospheric

pressure. The fluid is assumed to

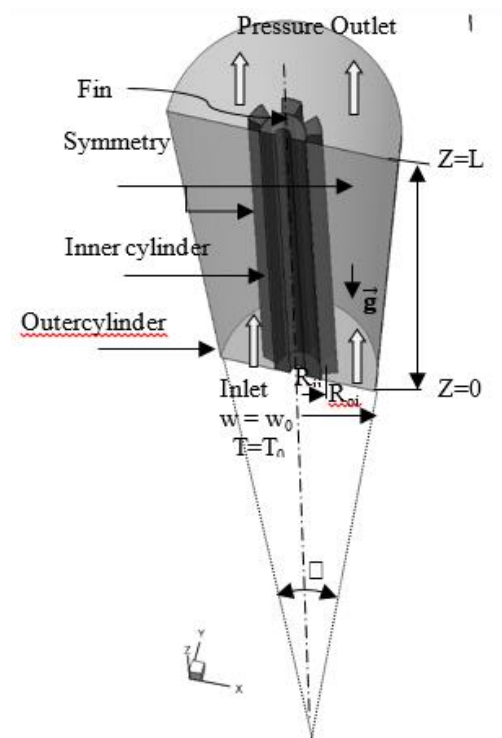


Fig. 1. Schematic view of the physical problem for $\phi=15^\circ$ and $N=3$.

be incompressible, viscous, and Newtonian having constant thermophysical properties except in the term of gravity where the Boussinesq assumption is adopted. The effect of viscous dissipation and radiation heat transfer are negligible. Table 1 shows the dimensions of the configuration.

Table 1 Dimensions of the studied configuration

Radius of inner cylinder (R_i)	3mm
Radius of inlet outer cylinder (R_{oi})	10 mm
Length of the duct (L)	5mm

2.1 Governing Equations

Considering of the simplifying assumptions formulated above, the governing equations in cylindrical coordinates in directions (r , θ , and z) are as follows:

- Continuity equation

$$\frac{1}{r} \frac{\partial(ru)}{\partial r} + \frac{1}{r} \frac{\partial v}{\partial \theta} + \frac{\partial w}{\partial z} = 0 \quad (1)$$

- Momentum equations

$$\left(\frac{1}{r} \frac{\partial(ruu)}{\partial r} + \frac{1}{r} \frac{\partial uv}{\partial \theta} + \frac{\partial uw}{\partial z} - \frac{v^2}{r} \right) = -\frac{1}{\rho} \frac{\partial p}{\partial r} + \frac{\mu}{\rho} \left[\frac{\partial}{\partial r} \left(\frac{1}{r} \frac{\partial}{\partial r} (ru) \right) + \frac{1}{r^2} \frac{\partial^2 u}{\partial \theta^2} - \frac{2}{r^2} \frac{\partial v}{\partial \theta} + \frac{\partial^2 u}{\partial z^2} \right] \quad (2)$$

$$\left(\frac{1}{r} \frac{\partial(ruu)}{\partial r} + \frac{1}{r} \frac{\partial uv}{\partial \theta} + \frac{\partial uw}{\partial z} - \frac{v^2}{r} \right) = -\frac{1}{\rho} \frac{\partial p}{\partial r} + \frac{\mu}{\rho} \left[\frac{\partial}{\partial r} \left(\frac{1}{r} \frac{\partial}{\partial r} (ru) \right) + \frac{1}{r^2} \frac{\partial^2 u}{\partial \theta^2} - \frac{2}{r^2} \frac{\partial v}{\partial \theta} + \frac{\partial^2 u}{\partial z^2} \right] \quad (3)$$

$$\left(\frac{1}{r} \frac{\partial(ruw)}{\partial r} + \frac{1}{r} \frac{\partial(vw)}{\partial \theta} + \frac{\partial(ww)}{\partial z} \right) = -\frac{1}{\rho} \frac{\partial p}{\partial z} + \frac{\mu}{\rho} \left[\frac{1}{r} \frac{\partial}{\partial r} \left(r \frac{\partial w}{\partial r} \right) + \frac{1}{r^2} \frac{\partial}{\partial \theta} \left(\frac{\partial w}{\partial \theta} \right) + \frac{\partial}{\partial z} \left(\frac{\partial w}{\partial z} \right) \right] - \rho g \beta (T - T_0) \quad (4)$$

• *Energy equation*

$$\frac{1}{r} \frac{\partial(ruT)}{\partial r} + \frac{1}{r} \frac{\partial(vT)}{\partial \theta} + \frac{\partial(wT)}{\partial z} = \frac{k_f}{(\rho C_p)} \left[\frac{1}{r} \frac{\partial}{\partial r} \left(r \frac{\partial T}{\partial r} \right) + \frac{1}{r^2} \frac{\partial^2 T}{\partial \theta^2} + \frac{\partial^2 T}{\partial z^2} \right] \quad (5)$$

• *Energy equation for solid wall*

$$\frac{k_s}{k_f} \left[\frac{1}{r} \frac{\partial}{\partial r} \left(\frac{\partial T}{\partial r} \right) + \frac{1}{r^2} \frac{\partial^2 T}{\partial \theta^2} + \frac{\partial^2 T}{\partial z^2} \right] = Q_v \quad (6)$$

The boundary conditions for this problem are:

The velocity boundary condition is (u =v=w=0) for the walls of the duct and the fins.

- For the fluid at inlet: T=T₀.
- For the adiabatic wall of the outer cylinder: at

$$z:(0,L) \quad \theta:(0,\pi) \quad \frac{\partial T(z,\theta,R)}{\partial r} = 0$$

- At interface solid-fluid

$$-\frac{\partial T}{\partial r} (R_{oi}, \theta, z) \Big|_{fluid} = K \frac{\partial T}{\partial r} (R_{oi}, \theta, z) \Big|_{solid}$$

K = k_s/k_f the thermal conductivity ratio

The parameter of natural convection is the Rayleigh number defined as function of the volumetric heat generation Q_v as:

K = k_s/k_f the thermal conductivity ratio

The parameter of natural convection is the Rayleigh number defined as function of the volumetric heat generation Q_v as:

$$Ra = \frac{g \beta Q_v \delta^5}{\nu \alpha k_f}$$

The local Nusselt number depends on the angular positions (Θ) and (z) expressed by the following equation:

$$Nu(z, \theta) = \frac{h_w(\theta, z) R}{k_f} = \frac{R}{k_f} \frac{1}{(T_w(R_f, \theta, z) - T_b(z))} \frac{\partial T}{\partial r} \Big|_{r=R_f} \quad (7)$$

With the mean Nusselt number defined as:

$$\overline{Nu} = \frac{1}{L} \int_0^L Nu(z) dz \quad (8)$$

T_w(R_f,Θ,z) is the local temperature of the wall, T_b(z) is the bulk temperature in the section (r - Θ).

$$T_b(z) = \frac{\int_0^{R_{oo}} \int_0^\pi T(r, \theta, z) r dr d\theta}{\int_0^{R_{oo}} \int_0^\pi r dr d\theta} \quad (9)$$

In order to study the effect of the fin on the average heat transfer rate for the heated wall of the inner cylinder, we introduce the average Nusselt number ratio NNR as referenced by(Prakash & Renzoni, 1985; Shi & Khodadadi, 2003) and it is defined as:

$$NNR = \frac{\overline{Nu}|_{withfin}}{Nu|_{withoutfin}} \quad (10)$$

A value of NNR greater than 1 indicates that the heat transfer rate is enhanced on the surface, whereas reduction of heat transfer is indicated when NNR is less than unity. The average Nusselt number can also be expressed via the hydraulic diameter D_hof the duct, the average heat transfer coefficient h_{avg} and the fluid thermal conductivity k_f of the fluid as follows:

$$\overline{Nu} = \frac{h_{avg} D_h}{k_f} \quad (11)$$

For a three-dimensional variable cross sectional area of the duct, the hydraulic diameter is defined based on the void volume between the inner and the outer cylinder. Shah *et al.*(1988). Such as:

$$D_h = 4 \frac{\text{void volume of the annulus}}{\text{welled surface area}} \quad (12)$$

For φ=0°

$$D_h = 4 \frac{L(6R_b^2 - N(R_f^2 - R_{ii}^2))}{(12(R_b L + R_b^2) - N(R_f^2 - R_{ii}^2))} \quad (13)$$

For φ>0°

$$D_h = 4 \frac{L(2(R_b^2 + R_t^2 + R_t R_b) - N(R_f^2 - R_{ii}^2))}{(6(R_b + R_t) \sqrt{L^2 + (R_t - R_b)^2} - N(R_f^2 - R_{ii}^2))} \quad (14)$$

Where R_b = R_{oi} - R_{ii}, R_t = R_{oo} - R_{ii}

The fin is an extended surface attached to the inner cylinder. Its cross section can vary depending on the distance r to the inner cylinder. The shaped of the fin used in this study is schematized in Fig. 2.

To determine the rate of heat transfer associated to the fin. The simplest procedure of the Fourier law(Park, Kim, & Kim, 2014) is assuming constant the thermal conductivity of the fin, the heat transfer by radiation is negligible and that the convective heat transfer coefficient is uniform along the wall of the fin.

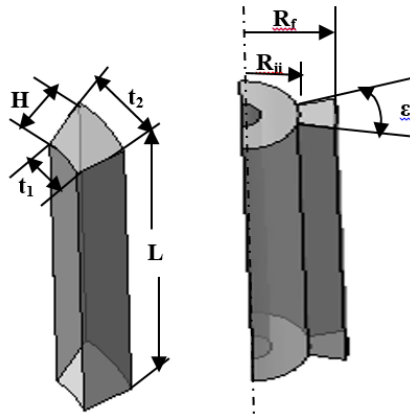


Fig. 2. Geometry of the fin.

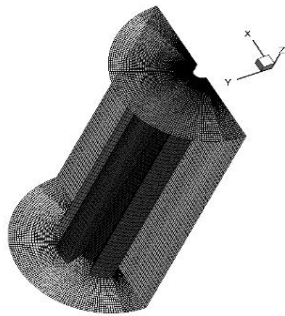


Fig. 3. Grid system for $\phi=0^\circ$, $N=3$.

The rate of heat transfer from a fin can be modeled as:

$$\dot{Q}_f = k_s m A_f (T_w - T_f) \cdot \tanh(m.H) \quad (15)$$

The parameter m is defined as:

$$m = \sqrt{\frac{h_{av} P}{k_s A_c}}$$

P is the perimeter and A_c is the cross-sectional area of the fin and are given by:

$$P = 2L + 2t_1, A_c = Lt_2$$

Also in terms of the convective heat transfer coefficient, the rate of heat transfer from that part of the base none occupied by fins \dot{Q}_b .

The heat transferred to air by convection can be determined by:

$$\dot{Q}_b = h_{av} A_b (T_w - T_f) \quad (16)$$

$$A_b = \pi LR_{ii} - N L t_1 \quad (17)$$

$$A_f = 2HL + 2Ht_2 + Lt_2 \quad (18)$$

$$t_1 = \frac{\alpha \pi R_{ii}}{180}, t_2 = \frac{\alpha \pi R_f}{180}$$

There for, the total rate of heat transfer

\dot{Q}_{tot} Which contain N fins can be expressed a

$$\dot{Q}_{tot} = N\dot{Q}_f + \dot{Q}_b \quad (19)$$

Using Eqs. (15), (16), (17) , (18) and (19), the thermal resistance can be modeled as:

$$R_{th} = \frac{(T_w - T_f)}{\dot{Q}_{tot}} = \frac{1}{h_{avg}(\eta NA_f + A_b)} \quad (20)$$

The thermal resistance is defined as the temperature difference between the inner cylinder temperature and the fluid temperature per unit heat flow and η is the fin efficiency.

3. NUMERICAL PROCEDURE

The governing equations associated with the boundary conditions were solved numerically by finite volume method using the commercially available software Fluent 6.3.26 (2006). The simple algorithm proposed by (Patankar, 1980) is used for coupling between pressure and velocity with a Power-Law approximation scheme. The convergence of the computational domain is determined on scaled residuals, for continuity, momentum and energy equations. The settings for all residuals for solution convergence, are 10^{-6} . The solution is considered to be converged if all residuals reach its default values. To reach the grid independent solution, three grids (30x99x25), (35x134x50), and (35x134x100) were tested for calculating the average Nusselt number Nu along the fin for $N=3, \phi=0^\circ$ and $Ra = 3.7 \times 10^3$ (Table 2) and Fig. 3.

Table 2 Grid independency test for $N=3, \phi=0$ and $Ra=3.7 \times 10^3$

Grids	30x99x25	35x134x50	35x134x100
\overline{Nu}	3.9493	3.9668	3.9898

In order to validate the presented numerical results, comparisons were made with those reported by (Elenbaas, 1942), (Churchill & Usagi, 1972), for parallel plates with different modified Rayleigh number Ra^* .

$$Ra^* = \frac{g \beta (T_w - T_0) \delta_{opt}^4}{\alpha \nu L}$$

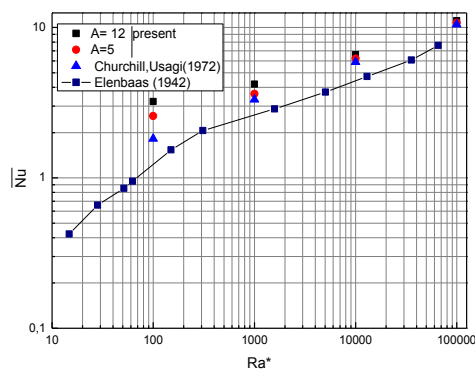


Fig. 4. Comparison between present results and those available in the literature.

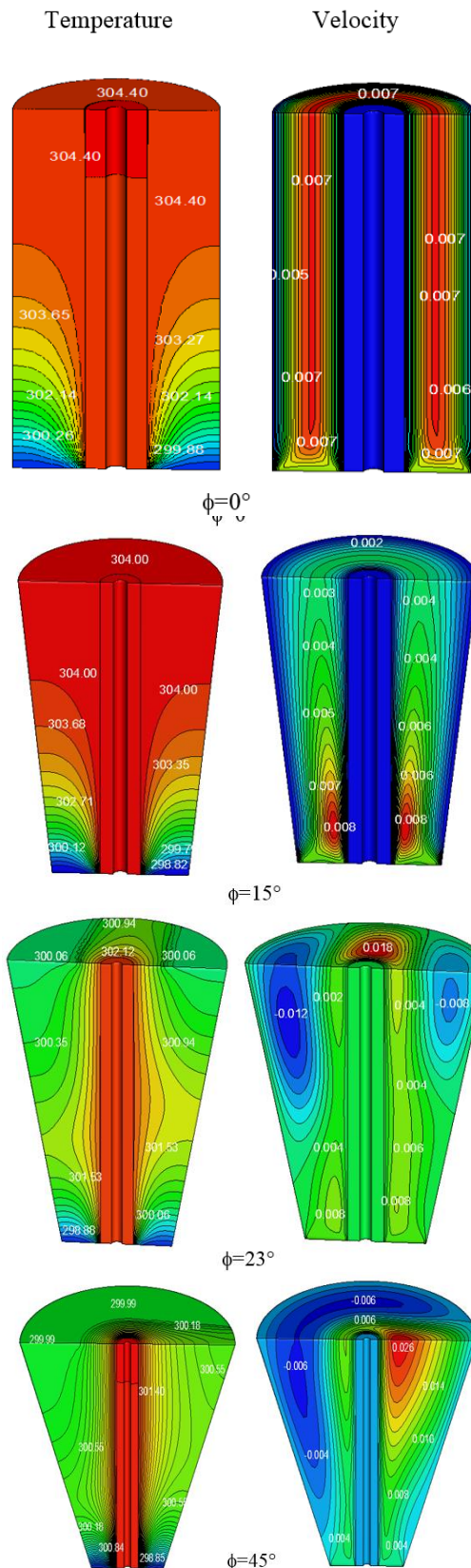


Fig. 5. Contour Fields of Temperature and Velocity, for $Ra=3.1 \times 10^4$ for $\phi=0^\circ, 15^\circ, 23^\circ$ and $\phi=45^\circ$ configurations without fin.

δ_{opt} is the optimum thickness between the plates for the aspect ratio ($A=5, A=12 (A=\delta_{opt}/L)$). It is seen from

Fig. 4 that the average Nusselt numbers are in good agreement.

4. RESULTS AND DISCUSSIONS

In this study, the natural convection flow in annular vertical duct is investigated numerically. The inner cylinder is subjected to a volumetric heat generation, while the wall of the outer cylinder is considered adiabatic. The characteristics of the flow and temperature field in the cylindrical and divergent duct are examined by exploiting the effects of above parameters like the inclination angle ϕ of the outer cylinder (divergent) and the fin characteristics, number of fins N , the high H and the angle between the fins γ . The numerical computations were performed for different physical

and geometrical parameters, the Rayleigh number ($Ra=1 \times 10^3$ to 1×10^5) and the inclination angle of the divergent ($\phi=0; 15^\circ; 23^\circ$ and 45°).

4.1 Influence of the Inclination Angle ϕ

The variation of the inclination angle of the divergent has an effect to change the structure of the flow in the contours fields of the temperature and the velocity. Figure 5, shows the contour fields in the span-wise direction of the flow, the temperature on the left, velocity on the right for a Raleigh number $Ra=3.1 \times 10^4$ and the inclination angle ($\phi=0^\circ; 15^\circ; 23^\circ$ and $\phi=45^\circ$) for a configuration without fins. This figure shows that the natural convection starts when the cold fluid enters the annular space between the two cylinders and changes its direction from the hot inner cylinder and moves towards the cold fluid and the outer cylinder. The temperature of the fluid increases in the direction of the main flow and reaches the maximum near the heated wall at the top. The thickness of the boundary layer increases as the flow moves up. For $\phi=0^\circ$ i.e. vertical cylinder, the fluid layers are concentric circles of which temperature decreases when moving away from the inner cylinder and the maximum temperature reached 304.36K. When the inclination angle of the divergent increases i.e. $\phi=15^\circ, 23^\circ$ and $\phi=45^\circ$ a variation in the structure of the isotherms was found, with a decrease of the temperature in the annular gap and the maximum temperature reached about 304K for $\phi=15^\circ, 300K$ for $\phi=23^\circ$ and 299K for $\phi=45^\circ$. Also, as depicted in this figure, the velocity contours show that the velocity decreases. Since the area at outlet is larger. For $\phi=0^\circ$ i.e. a vertical cylinder, the velocity fields show the existence of a symmetrical cell on both sides of the median plane of the duct where the highest velocities are concentrated in the middle of the annulus. For $\phi=15^\circ$ the size of this cell decreased, it is concentrated in the middle of the annulus near the entry where the velocity is raised. For $\phi=23^\circ$, the cell size is changed and it is localized in the top at the outlet. Then from this figure it can be seen that the temperature decreases and the velocity increases in the plume cell with the increasing of the inclination angle of the divergent and for the different inclination angle ϕ . Figure 6 depicts the variation of the average Nusselt number in versus of the Rayleigh number. It is observed that the increasing of the

inclination angle causes enhancement of the average Nusselt number. On the other hand, the average Nusselt number increases by increasing the Rayleigh number. Then the Nusselt number is influenced by the aperture angle of the divergent, by changing this angle the heat transfer produced is affected.

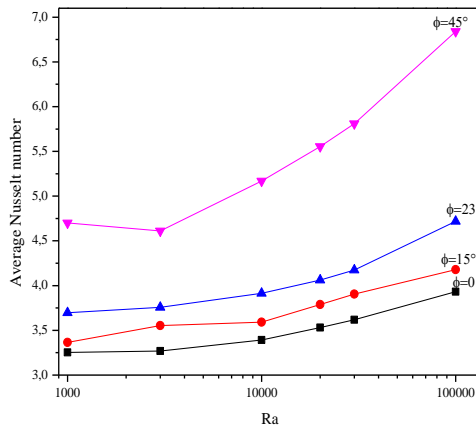


Fig. 6. Evolution of average Nusselt number as a function of Ra for various ϕ .

At $\phi=45^\circ$, this cell is larger and is concentrated towards the top on the right side of the duct.

Our numerical results can be correlated for the average Nusselt number. The expression of this correlation depends upon the Rayleigh number and the aperture angle ϕ and takes the form:

$$\overline{Nu} = A.Ra^B \tag{21}$$

Such that for:

$$\phi = 0^\circ, \overline{Nu} = 5.58 \cdot \left(\frac{2(R_{oo} - R_{oi})}{L} \right) Ra^{0.04289}$$

$$\phi = 15^\circ, \overline{Nu} = 24.2 \text{tg} \left(\frac{\phi}{2} \right) Ra^{0.0451}$$

$$\phi = 23^\circ, \overline{Nu} = 12.3 \text{tg} \left(\frac{\phi}{2} \right) Ra^{0.0532}$$

$$\phi = 45^\circ, \overline{Nu} = 7.71 \text{tg} \left(\frac{\phi}{2} \right) Ra^{0.09}$$

4.2 Influence of the Fin Parameters

The thermal resistance is defined as the temperature difference between the inner cylinder temperature and the fluid temperature per unit heat flow. Some calculated thermal resistance values are summarized in Table 3. To see the effect of the fin parameters as the fin numbers N and the height H on flow structure and heat transfer, we have presented the variation of the fin numbers N as function of the angle γ between it i.e. $N = 2, 3, 4$ correspond respectively to $\gamma=90^\circ, 60^\circ$ and $\gamma=45^\circ$ as shown in Fig. 7.

Table 3 Thermal resistances and temperature difference for various fin numbers, volumetric heat generation and inclination angle

$\phi(^{\circ})$	N	$Q_v(\text{W/m}^3)$	$R_{th}(\text{K/W})$	$T_w-T_0(\text{K})$
0°	1	1601	2.299	0.606
		16018	2.264	6.091
		5×10^5	1.859	187.85
	2	1601	1.132	0.555
		16018	1.118	5.570
		5×10^5	0.939	172.529
	3	1601	0.670	0.765
		16018	0.710	5.633
		5×10^5	0.618	167.421
15°	1	1601	2.052	0.602
		16018	1.998	6.042
		5×10^5	2.758	56.733
	2	1601	1.000	0.551
		16018	0.999	5.508
		5×10^5	0.999	171.931
	3	1601	0.627	0.3199
		16018	0.622	3.204
		5×10^5	0.652	100.153
23°	1	1601	1.972	0.600
		16018	2.676	4.359
		5×10^5	2.873	52.764
	2	1601	0.952	0.548
		16018	1.324	4.144
		5×10^5	1.286	48.337
	3	1601	0.6001	0.508
		16018	0.6005	5.085
		5×10^5	0.6004	158.754
45°	1	1601	2.031	0.598
		16018	3.124	4.078
		5×10^5	2.945	50.428
	2	1601	0.963	0.545
		16018	1.461	3.799
		5×10^5	1.429	45.621
	3	1601	0.618	0.6179
		16018	0.904	3.670
		5×10^5	0.837	43.517

Figure 8 displays contour fields of velocity and temperature on the plan $(r-\theta)$ on the cross sectional plan at the outlet of the duct for the following parameters. $Ra=3.1 \times 10^4$. ($\phi=45^\circ, N=2; 3; 4$ and $H=0.003\text{m}$). ($\phi=15^\circ, H=0.001\text{m}; 0.003\text{m}; 0.005\text{m}$ and $N=3$). The velocity and temperature contours are presented in the left and right half of the duct, respectively. As shown, for the same inclination angle ϕ ($\phi=45^\circ$), the influence of the number of fins is not significant. For $\phi=15^\circ$ the velocity and temperature contour fields are presented for the angle between the fins $\gamma=60^\circ$ i.e. $N=3$ for the values of the height of the fin respectively $H=0.001\text{m}, 0.003\text{m}$ and $H=0.005\text{m}$. It is shown that both velocity and temperature decreases as the height increases, a little

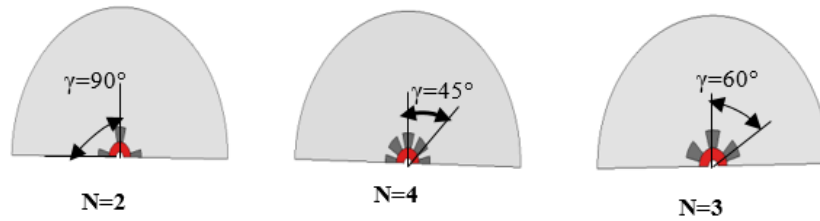


Fig. 7. Aperture angle and fins arrangement.

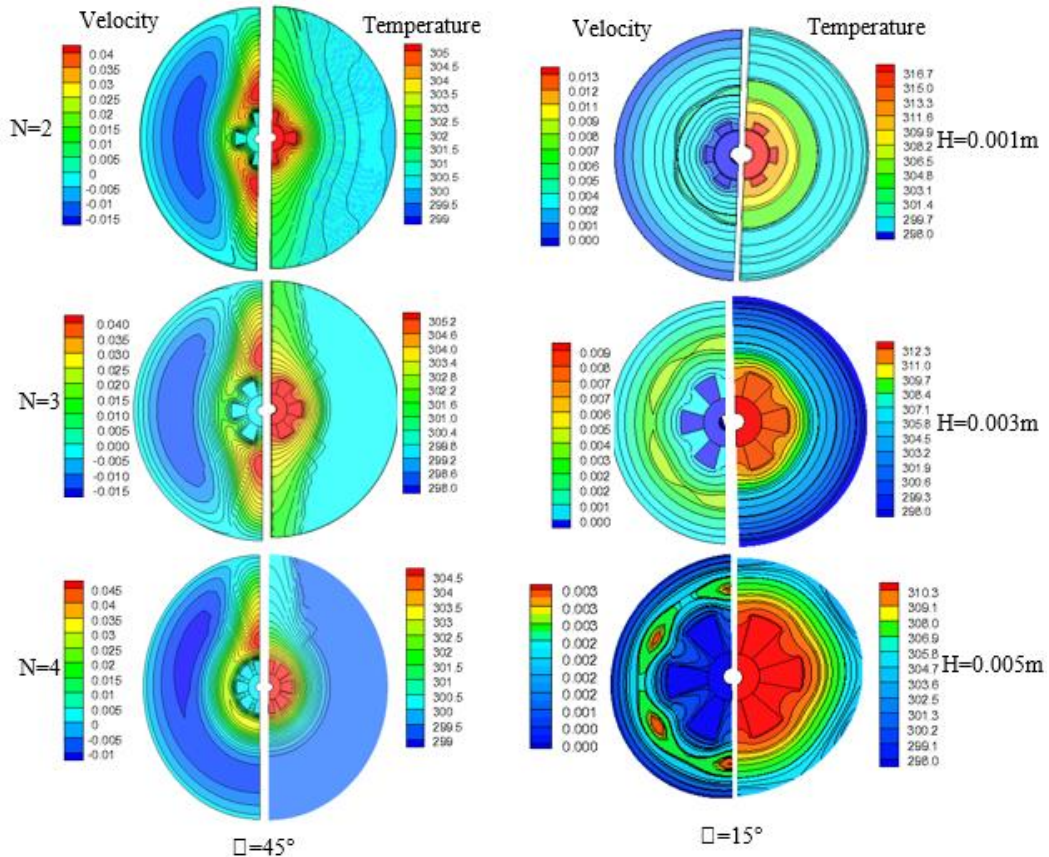


Fig. 8. Contour of velocity (the left half of the section) and temperature (the right half of the section) at outlet of the duct on the (r- θ) cross sectional plane for $Ra=3100$, $\phi=45^\circ$, $\phi=15^\circ$

plume cells are observed in this section when H increases, these plume cells are the location of the highest velocities. In other hand the temperature contours are concentric circles which temperature decreases away from the fin, this temperature reaches approximately the value 316K for $H=0.001m$, 312K for $H=0.003m$ and about 310 for $H=0.005m$, then the heat transfer is enhanced when H is increased. For $\phi=45^\circ$ and $N=2,3,4$, the negative values of the velocity show the recirculating zone and the zero values display the stagnant layer.

For $N=2$ and $N=3$ the temperature is higher and the recirculation zone is larger, hence the flow intensity is negligible. For $N=4$, the increasing of the velocity is only about 11% and the decreasing of the temperature is about 1.3%, this decreasing of temperature is caused by more fins. This is also shown in Fig. 9 which displays the temperature in the stream wise direction of the flow in a vertical line

near the fin for $\phi=45^\circ$ for the height of the fin $H=0.003m$ and $H=0.005m$. From this figure, it is seen that the plots have similar trends for the two values of H . Figure 9 shows the temperature and the local heat flux as a function of the axial direction z , for different fin height; for $\gamma=60^\circ$ (i.e. $N=3$); for $\phi=15^\circ$ and $\phi=45^\circ$. The figure reveals that the temperature increases at the duct entrance and attains a maximum point after which it becomes constant. The maximum temperature in the curves represents the starting of the fully developed thermal boundary layer, this increase in temperature is due by the dominance of the phenomenon of natural convection.

Also shown in Fig. 10 the local heat flux across the fin, which is another important heat transfer quantity of the problem under consideration. It can be seen from the figure that the local heat flux decreases from inlet to outlet, it is higher for lower fin heights. Also, its values for $\phi=45^\circ$ are lower compared to those for

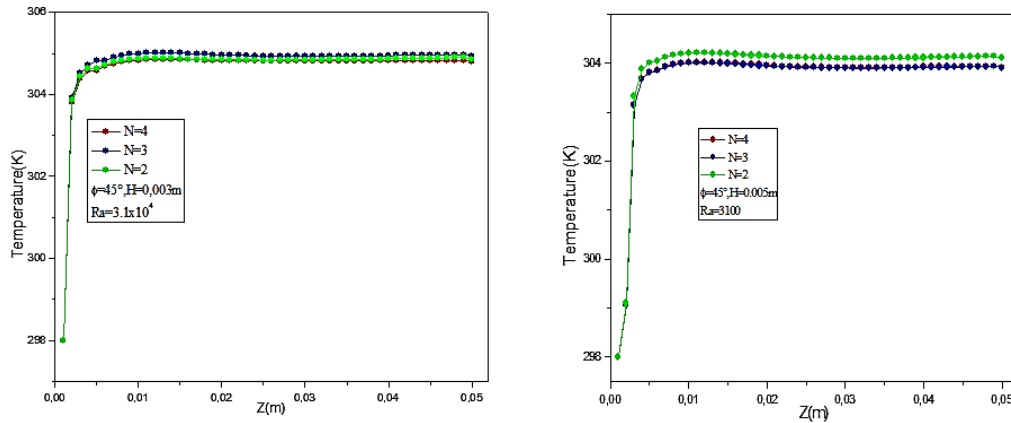


Fig. 9. Effect of fin numbers on the temperature of the fluid near the fin.

$\phi=15^\circ$, then the increasing of the inclination angle ϕ tends to result in a reduction of the temperature as well as the local heat flux and highest fins have to enhance the heat transfer in the duct. In Fig. 11, for the inclination angles ϕ cited above and the number of fins $N=1, 2$ and 3 , variations of the ratio NNR with the Rayleigh number are depicted. NNR increases when inclination angle ϕ increases, all the values of NNR are greater than 1 this indicates that the heat transfer is enhanced, for all the configurations and when Ra is less to 31000 NNR decrease. The rate of heat transfer is better for a number of fins $N=3$ and the inclination angle $\phi=45^\circ$. The NNR ratio for the different configurations can be correlated as function of the Rayleigh number in the form:

$$NNR = a.Ra^b \tag{22}$$

Table 4 shows the constants a, b and the errors for the inclination angle ϕ and the number of fins N considered.

Table 4 NNR correlation coefficients

$\phi=0^\circ$	N=1	N=2	N=3
a	0.787	1.127	1.800
error	0.216	0.328	0.473
b	0.071	0.054	0.054
error	0.032	0.035	0.032
$\phi=15^\circ$	N=1	N=2	N=3
a	1.116	0.865	1.438
error	0.042	0.322	0.432
b	0.009	0.099	0.081
error	0.004	0.042	0.035
$\phi=23^\circ$	N=1	N=2	N=3
a	1.202	1.510	2.086
error	0.049	0.521	0.658
b	-2.8×10^{-4}	-3.6×10^{-4}	0.015
error	0.005	0.045	0.040
$\phi=45^\circ$	N=1	N=2	N=3
a	0.863	0.979	1.268
error	0.254	0.583	0.665
b	0.049	0.074	0.100
error	0.035	0.070	0.060

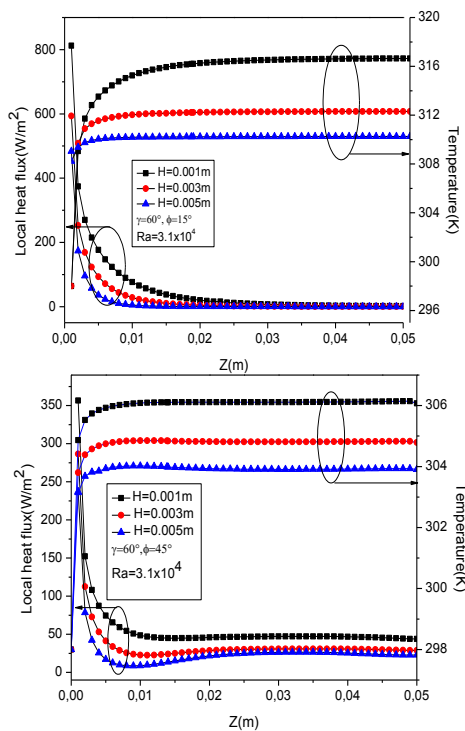


Fig. 10. Effect of fin height on the temperature and the local heat flux for $\phi=15^\circ$ and $\phi=45^\circ$.

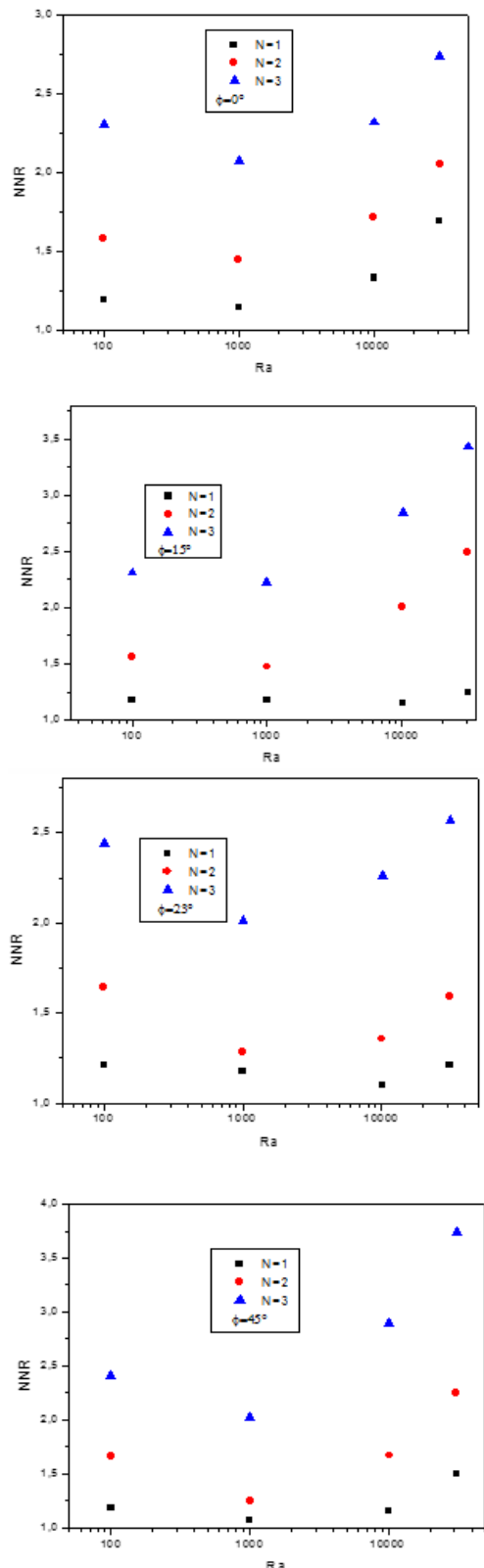


Fig. 11. Variation of the ratio NNR via Ra, ϕ and N.

5. CONCLUSION

In this study, the 3D natural convection in annular cylindrical and divergent duct was investigated

numerically. The effect of the inclination angle of the divergent and the fin parameters in the structure of the flow and the heat transfer are considered. The governing parameters are ϕ , Ra and N. The results of this study show that for a given Rayleigh number, the results of this study show that for a given Rayleigh number, the temperature decreases and the velocity increases with increasing the inclination angle of the divergent. High inclination angle yields significant heat transfer of a fixed fin and Rayleigh number and tends to result in a reduction of the temperature as well as the local heat flux. Also, highest fins have to enhance the heat transfer in the duct.

Correlation of results for the average Nusselt number ratio was obtained, further there is no prior literature dealing with a generalized correlation for average Nusselt number ratio in annular divergent duct fitted with fins.

REFERENCES

- An, B. H., H. J. Kim and D. K. Kim (2012). Nusselt number correlation for natural convection from vertical cylinders with vertically oriented plate fins. *Experimental Thermal and Fluid Science* 41, 59-66.
- Benkherbache, S. and M. SI-Ameur (2016). Natural convection in a cylindrical and divergent annular duct fitted with fins. *International Journal of Energy, Environment and Economics* 24(4), 503-518.
- Churchill, S. and R. Usagi (1972). A general expression for the correlation of rates of transfer and other phenomena. *AIChE Journal* 18(6), 1121-1128.
- Elenbaas, W. (1942). Heat dissipation of parallel plates by free convection. *Physica* 9(1), 1-28.
- Kumar, R. (1997). Three-dimensional natural convective flow in a vertical annulus with longitudinal fins. *International Journal of Heat and Mass Transfer* 40(14), 3323-3334.
- Li, B. and C. Byon (2015). Orientation effects on thermal performance of radial heat sinks with a concentric ring subject to natural convection. *International Journal of Heat and Mass Transfer* 90, 102-108.
- Park, K. T., H. J. Kim and D. K. Kim (2014). Experimental study of natural convection from vertical cylinders with branched fins. *Experimental Thermal and Fluid Science* 54, 29-37.
- Patankar, S. (1980). *Numerical heat transfer and fluid flow*: CRC press.
- Prakash, C. and P. Renzoni (1985). Effect of buoyancy on laminar fully developed flow in a vertical annular passage with radial internal fins. *International Journal of Heat and Mass Transfer* 28(5), 995-1003.
- Shi, X. and J. Khodadadi (2003). Laminar natural convection heat transfer in a differentially

- heated square cavity due to a thin fin on the hot wall. *Journal of Heat Transfer* 125(4), 624-634.
- Shah, R. K., Subbarao, E. C., Mashelkar, R. A. (1988). *Heat Transfer Equipment Design Book Review*. Hemisphere Publishing Corp., New York, U.S.A.
- Starner, K. and H. McManus (1963). An experimental investigation of free-convection heat transfer from rectangular-fin arrays. *Journal of Heat Transfer* 85(3), 273-277.
- Toshio, A.. (1970). Natural Convection Heat Transfer from Vertical Rectangular-Fin Arrays: Part 2, Heat Transfer from Fin-Edges. *Bulletin of JSME* 13(64), 1182-1191.
- Yu, S. H., D. Jang and K. S. Lee (2012). Effect of radiation in a radial heat sink under natural convection. *International Journal of Heat and Mass Transfer* 55(1-3), 505-509.
- Yu, S. H., K. S. Lee and S. J. Yook (2010). Natural convection around a radial heat sink. *International Journal of Heat and Mass Transfer* 53(13-14), 2935-2938.
- Yu, S. H., K. S. Lee and S. J. Yook (2011). Optimum design of a radial heat sink under natural convection. *International Journal of Heat and Mass Transfer* 54(11-12), 2499-2505.